

Numerical Simulation of Composite Precast Concrete Girders

Wael Nabil^{1*}, Ayman Khalil², Sherif Elwan³

¹Ph.D. Candidate, Department of Structural Engineering, Faculty of Engineering, Ain Shams University, Cairo, Egypt

²Professor, Department of Structural Engineering, Faculty of Engineering, Ain Shams University, Cairo, Egypt

^{1,3}Department of Civil Engineering, The Higher Institute of Engineering – El Shorouk Academy, Cairo, Egypt

Abstract: ABAQUS software was used in a finite element analysis (FEA) to analyze the behavior of composite precast concrete beams the behaviour of composite precast concrete beams, ABAQUS software was used in a finite element analysis (FEA). This study aims to present a model that can be used to analyze composite precast concrete beams with finite element techniques. Concrete is a widely used material in civil structures and many architectural, and it behaves differently in compression and tension as well as nonlinearly elastically. Concrete's characteristics make it challenging to model or simulate the substance. An issue with the bond-slip relationship between concrete and steel in reinforced concrete is particularly problematic. However, certain presumptions were made in this study, such as the perfect bond between the steel and concrete and the concrete damage plasticity (CDP) model for concrete properties, when performing the finite element analysis for composite concrete beams through ABAQUS simulation. When comparing analysis and experimental results, simulated tensile deformations closely resemble the actual crack patterns found in tests. The crack pattern is provided by a finite element model that exhibits the same trend in the load-displacement relation as the experimental ones.

Keywords: Finite element method, concrete damage plasticity, composite concrete, numerical simulation.

1. Introduction

Due to their ability to provide high spans with relatively small dimensions, composite precast concrete beams are increasingly being used in residential buildings, commercial buildings, towers, and bridges today. It has always been difficult to decide which approach to use when using finite element models to simulate the pre-compression force in the tendons. A variety of studies were done to compare different tendon modeling approaches. Three modeling approaches, including tube-to-tube, multiple spring systems, and surface-to-surface contact, were listed by Kang et al. [1] as ways to simulate post-tensioned beams. They compared these techniques with experimental tests and discovered that while all three are workable, the third is the most trustworthy. Although the computational time for the first two methods was much longer than for the surface-to-surface method, they produced results that were extremely accurate.

In their study of the slip behaviour of tendons on concrete

surfaces, Kwak et al. [2] compared analytical as well as experimental studies. It demonstrates the effective modeling for the prestressed concrete beam in ADINA, as well as very similar results to the experimental results that have been shown. Nonlinear analysis is necessary to analyze the slip-in tendons because the anchorage and top face of concrete may exhibit nonlinear behaviour.

S.V. Chaudhari and others [3] When comparing stress-strain curves for various mesh sizes, it was discovered that using CDP requires a smaller mesh size to achieve the desired accuracy. Because modeling prestressed reinforcement with volumetric elements takes a lot of computation time, Arab, A., et al. [4] compared two models: one that used the embedding method, in which truss elements were utilized to simulate prestressed reinforcement and the other that used the extrusion technique, in which the surface to the surface method was used. Comparative analysis of the data and the outcomes of the experiment was used to further validate both methods. The researchers concluded that the embedded method, as opposed to the volumetric method, offers an accurate, and numerically effective alternative when simulating prestressed tendons in concrete beams. Few studies have examined the best ways to prestress tendons up to this point.

Even when a structure's stress level is deemed "perfect," failures of its components can occasionally result in cracks that can have disastrous consequences. The investigation of crack initiation and spread is a challenging topic. In the field of fracture mechanics engineering, determining the primary scenario involving the spread of cracks is taken into consideration. We can create a potent and trustworthy analytical technique, like the finite element method (FEM), because the cost and the time of otherwise expensive experimental tests are reduced. The deformation, support conditions, and loading of the actual experimental test may be more accurately simulated by the finite element method. For instance, engineers want to comprehend the circumstances under which a pre-existing crack continues to spread. After that, other fracture mechanics-related characteristics were investigated and the stress at the tip of a pre-crack was determined using Finite Element Analysis (FEA). As a result, the ABAQUS finite element analysis software's FM module is used.

*Corresponding author: w.nabil@sha.edu.eg

2. Experimental Work

A. Specimen Details

Information about the tested beam in detail is shown in Fig. 1.

The beam had a clear span of 4.2 m and a 100 mm projection on each side. To design bridge girders, it was deemed necessary to test beams with a suitable and typical span-to-depth ratio. The beam had a depth of 400 mm and a breadth of 120 mm; hence the span-to-depth ratio was 10.5, which is considered a typical value in practice. The flange width was 1000 mm. The beam was prestressed with a standard 0.6-inch steel strand, The prestressed strands were positioned through the beam span with a polygon profile, as shown in Fig. 1 to decrease the eccentricity at supports to avoid tension stresses at the beam ends. The polygon edges were curved to reduce friction losses. Besides prestressed reinforcement.

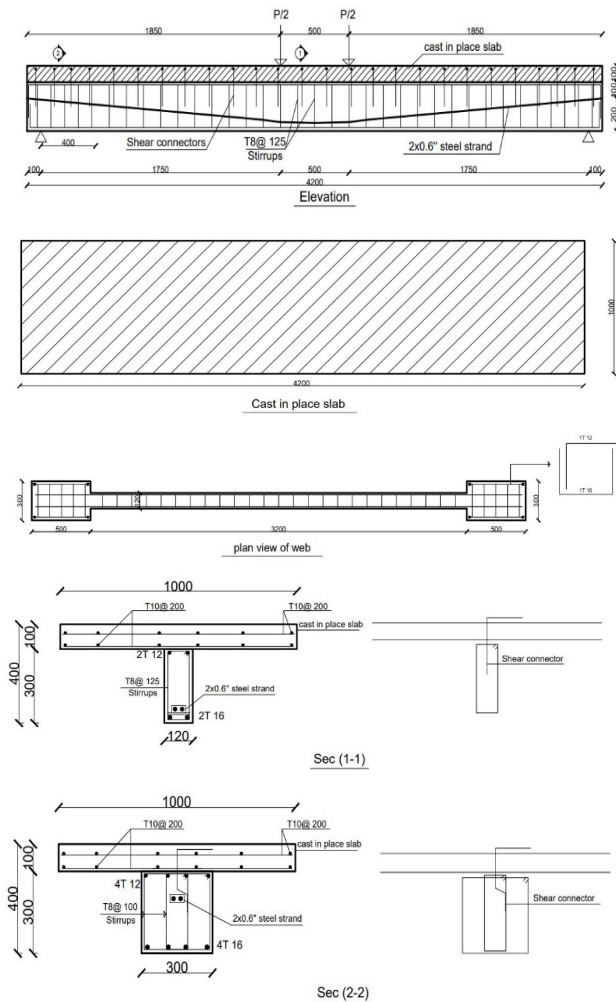


Fig. 1. Details of the specimen

Two longitudinal steel bars of 12 mm diameter and 16 mm diameter were used to reinforce the beam at the top and bottom, respectively. The beam was reinforced for shear using rectangular stirrups, with a diameter of 8 mm, uniformly distributed every 100 mm through the first and last 0.5 m, and

between them uniformly distributed every 125 mm, as shown in Fig. 1. In the first 500 mm of the beam, two more stirrups were added to avoid any excessive stresses from the prestressing force. The stirrups were tied to two top longitudinal steel bars, 10 mm in diameter. The yield stress for stirrups was 240 MPa, and the top steel bars were 400 MPa. The flange was reinforced with a 10 mm bar at 200 mm spacing in both sides. The shear reinforcement of the beam was designed with an adequate safety factor to force and guarantee a Separation failure of the specimen.

B. Material Properties

The mix of concrete was created using locally manufactured ordinary Portland cement, sand, and finely crushed stones. In addition, a liquid set retarding concrete admixture with a plasticizing effect to achieve a water reduction without loss of workability was used and designed to obtain a cylinder concrete strength of 40 MPa at 28 days. The mixes proportions by weight are shown in Table 1. For control purposes, six concrete cubes with dimensions 150 x 150 x 150 mm and six cylinders with 300 mm height and 150 mm diameter were cast alongside the specimen from the same concrete batch and were cured with the specimen, as shown in Fig. 2.



Fig. 2. Concrete cubes testing

Moreover, 6 prisms with dimensions equal to 100x100x500 mm, for width, height and length respectively, were also cast in order to test the concrete tensile strength, as shown in Fig. 3. The cubes, cylinders, and prisms were tested on the same day as testing the beams. Table 3 shows the cube concrete and the cylinder compressive strength, and the tensile strength of the specimen.

Materials	Mix (40Mpa)
Cement (Kg)	38.70
Sand (Kg)	56.40
Fine gravel (Kg)	84.71
Water (liter)	13.54
Superplasticizer	0.58



Fig. 3. Concrete prisms testing

Table 2
Concrete compressive and tensile strength

Cylinder Compressive Strength (Mpa)	36.7
Cube Compressive Strength (Mpa)	42.20
Obtained Tensile Strength from Testing (Mpa)	6.28

The grout was injected through the corrugated plastic ducts holding the prestressing steel as depicted in Fig. 4 at a rate of 500gm/100kg cement in the grout. Figures 5 and 6 depict prisms that were cast to investigate the compressive and tensile strength of the grout.



Fig. 4. Grouting process



Fig. 5. Grout prisms



Fig. 6. Compressive strength test of grout prism

Non-prestressed steel is used in reinforcement cages. High-strength steel bars with a 10 mm diameter and 400 MPa yield stress were used for main reinforcement, and mild steel bars with an 8 mm diameter and 240 MPa yield stress were used for stirrups.

Uncoated seven-wire strands grade 1860, low relaxation, with two main nominal diameters of 0.6 inch were used according to the specimen design as shown in Fig. 7. These strands followed the ASTM International (2002) standard specifications. The steel area of the strand was 140 mm², with a grade of 1860 MPa, and the elastic modulus was 195000 MPa. According to the specifications the 0.6-inch strand is designated as strand no. 15 has a minimum load of 234 kN at 1 % extension for low relaxation cables.



Fig. 7. Seven wire strand

C. Casting of the Specimen

The specimen was fabricated in two phases; the first phase was the fabrication of the post-tensioned concrete web, and the second stage was casting the top slab. The post-tensioned concrete web was fabricated as follows, the forms were prepared for casting the concrete, Steel reinforced cages were prepared and details of the anchorage zone were made, the duct with the strand inside it was installed the prestressing beam presenting the cable profile designed and fixed the cages by small steel pieces, the grouting fitting was attached to the duct with small vertical tube comes out of concrete beam surface for grout injecting, The cage with the duct was placed in the wooden forms, The concrete was cast, as shown in Fig, 8 and

compacted with electrical vibrator for three minutes, and during of the specimen with water started immediately after the initial setting of concrete for seven days.



Fig. 8. Casting beam

D. Application of Prestressing Force

As shown in Fig. 9, the prestressing force was applied 28 days after the concrete was cast using a 250 kN capacity jack with locking nuts to maintain the force after jacking. The load was applied in increments of 25 % at each time on each beam end. the application of prestressing force was as follows, make a marker on the strand on both sides to be able to measure elongation after tensioning the cable and tensioning the strand from one end approximately 25% of the required force than 50%,75% and 100% of required force, as shown in Fig. 10, and measure the final elongation and calculate the required force to make this elongation. It is noted that the tendons were tension by force at was level of 75 % of the ultimate strength.



Fig. 9. The jack using for tensioning tendons



Fig. 10. Elongation after tensioning the tendon

E. Application of Prestressing Force

After transferring the prestressing force to the tendon, the grout was injected under pressure into the duct around the strand using the grouting machine shown in Fig. 11, as shown in the following steps, preparing the grout by adding 50 kg of cement and 5 kg of grout powder to 23 litter of water in the grouting machine, inject the grout under pressure using the grouting machine into the vertical tube of the duct into the pre-stressing beam, as shown in Fig. 12, keep injecting the grout from one end till it comes out from the other end to ensure that the grout fills the duct completely.

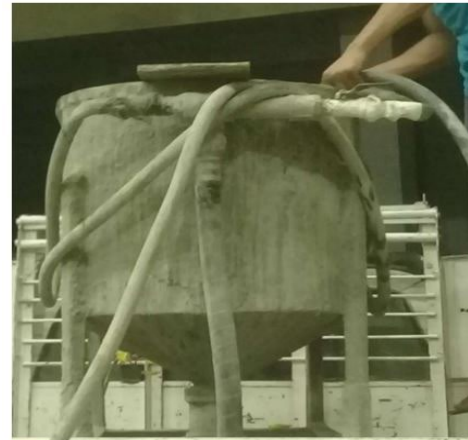


Fig. 11. Grouting machine



Fig. 12. Grouting injection

F. Test Setup

Testing was done using the testing frame in the concrete testing lab of the Faculty of Engineering at Ain Shams University. The test subject was put through a four-point loading scenario with a constant moment zone. This set up must be accomplished using a 1000 kN hydraulic jack and a 1000 kN load cell. To achieve the two-acting loads, the applied load is split into two-point loads using a rigid steel spreader beam with a length of 1.00m. The rigid steel beam was supported by a

30mm steel plate that sat atop the concrete beam. A mortar-based material is used to secure this 30mm steel plate to the concrete surface. The steel plate is then levelled with a spirit level to ensure that it is horizontal. The test setup and loading system are depicted in Figure 13.



Fig. 13. Test setup

3. Finite Element Model

The general-purpose FE software ABAQUS was used to build and analyze a FE model for a post-tensioned concrete beam. A 4-node bilinear shell element (CPS4R) for concrete, and a 2-node linear 2-D truss element (T2D2) for internal reinforcements. As a result of the sensitivity study for mesh size, a mesh size of about 20 mm was suggested in this study, as shown in Fig. 14.

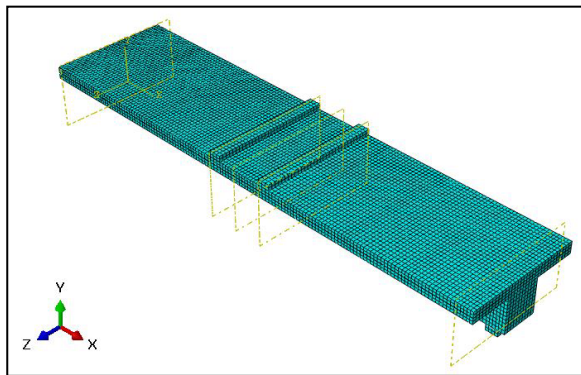


Fig. 14. 3D modeling of mesh size

Concrete and internal reinforcements were combined using the 'Embedded' command for modeling simplicity, with the assumption that the internal bars are perfectly bonded to the concrete during the theoretical section analysis. The 'surface-to-surface' command was used for the contact between the concrete bottom and saddle pin, the concrete hole and anchor pin, and the pin and saddle plate. As contact interaction properties, "Hard" contact in normal behaviour and a common friction coefficient of 0.3 in tangential behaviour were considered. Both steel rod ends in the tests had bolt threads and were connected to clevis or nuts, but they were not modelled because their modelling required time, and this analysis was conducted in two-dimensional elements. Instead of detailed modelling, two joints were combined using an 'Equation'

command. This simplification appears to be suitable because thread failure is not the primary mode of failure in this study. The distance between contact elements was set to 'zero' to avoid analytical difficulties when the simulation began.

A. Modeling of Concrete

ABAQUS has a "Concrete Damaged Plasticity (CDP)" option for analyzing concrete damage. The dilation angle (ψ), flow potential eccentricity (e), a ratio of the compressive strength under biaxial loading to that under uniaxial loading (f_b/f_c), a ratio of the second stress invariant on the tensile meridian to that on the compressive meridian (K), viscosity parameter (η), elasticity modulus of concrete (E_c), concrete compressive behaviour, and concrete tensile behaviour are the main parameters considered in this study. According to the ACI code, $E_c = 4700 \sqrt{f_c}$, where f_c was measured from a compressive strength test and is in MPa. The flow potential eccentricity (e) was set to the default value of 0.1. Because the equibiaxial strength of concrete (f_{b_0}) was not measured in the experimental work and is rare in other studies, the equation of $f_b/f_c = 1.5 (f_c)^{-0.075}$ proposed by Tao et al. [21] and Papanikolaou and Kappos [22] were cited in this model. f_{c_0} is the same symbol as f_c in ACI code. The yield surface of the concrete is determined by the ratio of the second stress invariant on the tensile meridian to the compressive meridian (K). According to Seow and Swaddiwudhipong [23], the range of K is between 0.5 and 1.0, but many other researchers have used the 2/3 default value. The equation $K = (5.5 f_{b_0}) / (2 f_c + 5 f_{b_0})$ proposed by Yu et al. [15] was used in this study. Both the dilation angle (ψ) and viscosity parameters have become important parameters in this study because they are highly sensitive to analysis and are scarce in other studies. In ABAQUS, the range for defining the plastic flow potential is 0° to 56° (Tao et al., [21]). A few researchers entered the various values but adopted them on a case-by-case basis. According to numerous sensitivity analyses, was chosen as 38° in this study. Its value had no effect on the initial behaviour of load-deflection but had a significant effect on plastic behaviour after elastic behaviour. The viscosity parameter (η) in ABAQUS/Standard analysis is used for the viscoelastic regularisation of the concrete constitutive equation, and it has a default value of zero. A value of zero could not be chosen for this study because the finite element analysis (FEA) did not continue in the elastic behaviour, even though Tao et al. [21] stated that it has no significant influence on prediction accuracy. The stress-strain relationship for concrete was based on the work of Hognestad [10] and Lou et al., [13], as shown in Figs. 15 and 16.

B. Modeling of Steel

Tensile tests were used to measure actual stress (σ) and strain (ϵ) data for steel materials such as reinforcement and external rods, which were then converted for use in ABAQUS software. Because the measured data are nominal stress-strain data, ABAQUS analysis requires a simple conversion to true stress and logarithmic strain as shown in Eqs. 1-2 (Dai et al., [9]).

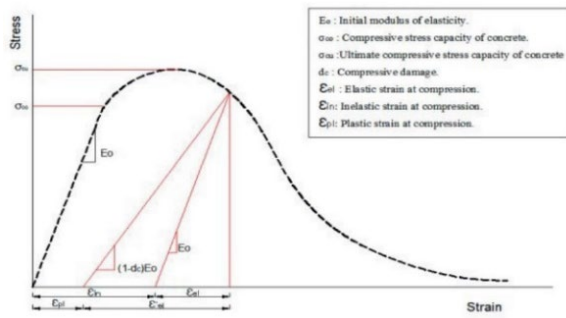


Fig. 15. Compressive behavior of concrete

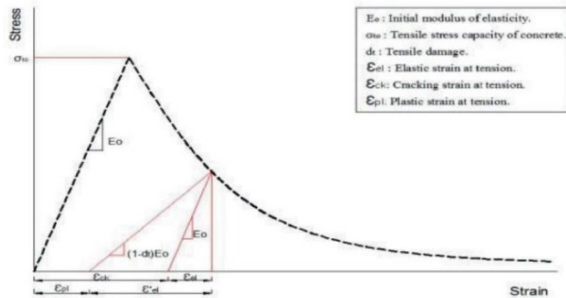


Fig. 16. Tensile behavior of concrete

4. Results and Discussion

Fig. 17 and Fig. 18 showed failure mode and crack pattern for the beams. Fig. 19 showed stress S11 in reinforcement. Fig. 20 and Fig. 21 showed the deformed shape of the beam.

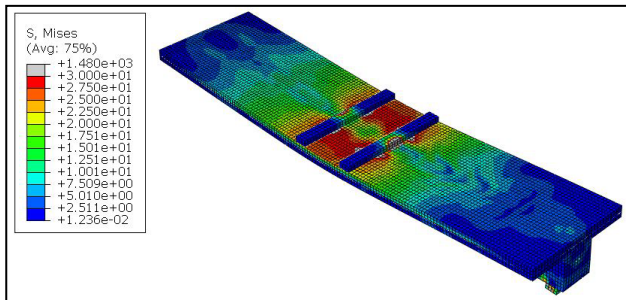


Fig. 17. Failure mode for the tested beam

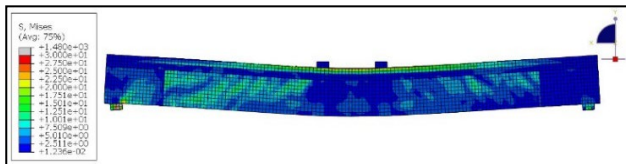


Fig. 18. Crack pattern for the tested beam

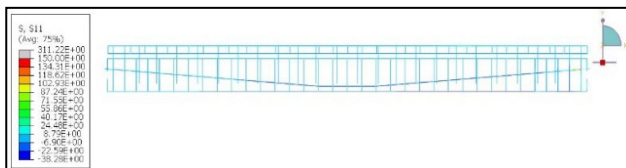


Fig. 19. Stress in reinforcement

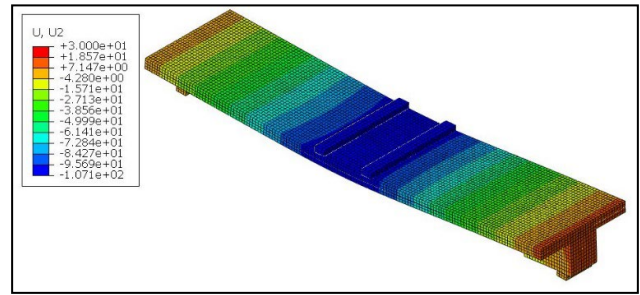


Fig. 20. 3D modelling of deformed shape for the tested beam

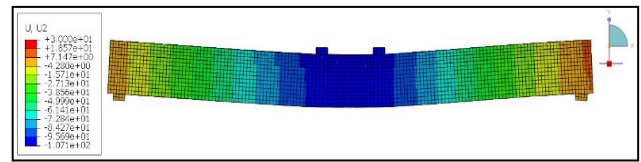


Fig. 21. Deformed shape for the tested beam

As shown in Fig. 22, the FE model agrees with the experimental test results in terms of deflection. Table 3 shows the ratio of the experimental failure load and FE models' ultimate load. The accuracy of the ultimate load capacity is validated in Table 3 with a value of 1.03% between the experimental test results and those obtained from FE models, indicating that good accuracy can be achieved when using this model for further combing them to handle experimental FE program for the composite Post-tensioned RC beams.

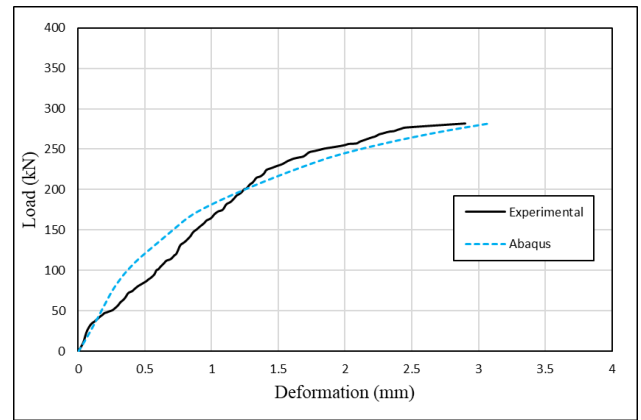


Fig. 22. Load-deflection curve of experimental and FE-modeled beam

Table 3
Comparison between the experimental failure load and FE model results

Experimental (kN)	FEM ABAQUS (kN)	Experimental / FEM ABAQUS
288	280	1.03

5. Conclusions

In this study, the concrete damage plasticity model was used to perform finite element analysis on a composite post-tensioned precast beam. The following conclusions can be drawn from the validation of the finite element model against experimental findings and parametric study with varied values of prestressing force, dilation angle, and viscosity parameter:

- 1) A nonlinear analysis of three-dimensional reinforced concrete beams subjected to concentrically increasing

- loads was created using the ABAQUS computer program to simulate the behaviour of experimental beams.
- 2) The concrete crushing failure mode in PPC panels can be predicted using the concrete damage plasticity model in ABAQUS. The mid-span displacement and failure loads' numerical errors were within 1.03% and 8%, respectively.
 - 3) The finite element model's predicted crack pattern is almost identical to the experimental ones and follows the same pattern for the load-displacement response.
 - 4) By comparing the CDP model predictions to the actual crack pattern, concrete tensile deformation can be accurately predicted.
 - 5) Based on the dilation angle (ψ), flow potential eccentricity (e), ratio of compressive strength under biaxial loading to compressive strength under uniaxial loading (f_b/f_c), ratio of second stress invariant on the tensile meridian to that on the viscosity parameter (μ), and compressive meridian (K) of CDP model, analytical results of strength and deflection are like those of the experimental results.
 - 6) Higher calculation time and accuracy were associated with lower values of the parameter's viscosity.

References

- [1] Kang, T., Huang, Y., "Computer Modeling of Post-Tensioned Structures", 4th International Conference on Computer Modelling and Simulation, vol. 22, pp. 41-45, 2012.
- [2] Kwak, H., Kim, J., and Kim, S., "Nonlinear analysis of prestressed concrete structures considering slip behavior of tendons", *Computers and Concrete*, vol. 3, no. 1, pp. 43-64, 2006.
- [3] Chaudhari, S.V., Chakrabarti, M.A., "Modeling of concrete for nonlinear analysis Using Finite Element Code ABAQUS", *International Journal of Computer Applications* (0975 – 8887), vol. 44, no. 7, pp. 14-18, April 2012.
- [4] Arab, A., Sameh, S., Badie, b., Majid, T. and Manzari, b., "A methodological approach for finite element modeling of pretensioned concrete members at the release of pretensioning", *Engineering structures*, vol. 33, no. 6, pp. 1918-1929, 2011.
- [5] Nikaido, Y., Mihara, Y., Sawada, S., Takahashi, Y., "Improvement and enhancement of concrete damage plasticity model", In *Proceedings of the Simulia Community Conference Proceedings*, Berlin, Germany, pp. 18–21, May 2015.
- [6] Zhang, C., Cao, P., Cao, Y., Li, J., "Using finite element software to simulation fracture behavior of three-point bending beam with initial crack", *J. Softw.*, vol. 8, no. 5, pp. 1145–1150, 2013, doi:10.4304/jsw.8.5.1145-1150.
- [7] Yin, Y., Qiao, Y., Hu, S., "Determining concrete fracture parameters using three-point bending beams with various specimen spans", *Theor. Appl. Fract. Mech.*, 107, 2020, 102465.
- [8] Chaudhari, S.V., and Chakrabarti, M.A. "Modeling of concrete for nonlinear analysis using finite element code ABAQUS", *International Journal of Computer Applications*, vol. 44, no. 7, pp. 14-18, 2012.
- [9] Dai, X.H., Wang, Y.C., and Bailey, C.G., "Numerical modelling of structural fire behaviour of restrained steel beam-column assemblies using typical joints types", *Engineering Structures*, vol. 32, no. 8, pp. 2337-2351, 2010.
- [10] Hognestad, E., "A study of Combined Bending and Axial Load in Reinforced Concrete Members", University of Illinois Engineering Experimental Station, IL, USA, 1951.
- [11] Jankowiak, T., and Łodygowski, T., "Identification of parameters of concrete damage plasticity constitutive model", *Foundation of Civil and Environmental Engineering*, vol. 6, pp. 53-69, 2005.
- [12] Kmiecik, P., and Kamiński, M. "Modelling of reinforced concrete structures and composite structures with concrete strength degradation taken into consideration", *Archives of Civil and Mechanical Engineering*, vol. 11, no. 3, pp. 623-635, 2011.
- [13] Lou, T., Lopes, S.M.R., and Lopes, A.V., "Flexural response of continuous concrete beams prestressed with external tendons", *Journal of Bridge Engineering*, vol. 18, no. 6, pp. 525-537, 2013.
- [14] Nazem, M.N., Rahimani, I., and Rezaee-Pajand, M., "Nonlinear FE analysis of reinforced concrete structures using a Treca-type yield surface", *Scientia Iranica*, vol. 16, no. 6, pp. 512-519, 2009.
- [15] Yu, T., Teng, J.G., Wong, Y.L., and Dong, S.L., "Finite element modeling of confined concrete I: Drucker-Prager type plasticity model", *Engineering Structures*, vol. 32, no. 3, pp. 665-679, 2010.
- [16] Scott, B.D., Park, R., and Priestly, M.J.N., "Stress-strain behavior of concrete confined by overlapping hoops at low and high strain rates", *ACI Structural Journal*, vol. 79, no. 1, pp.13-27, 1982.
- [17] Seow, P.E.C, and Swaddiwudhipong, S., "Failure surface for concrete under multiaxial load – a unified approach", *Journal of Materials in Civil Engineering*, vol. 17, no. 2, pp. 219-228, 2005.
- [18] Wang, T., Hsu, T.T.C., "Nonlinear finite element analysis of concrete structures using new constitutive models", *Computers and Structures*, vol. 79, no. 32, pp. 2781-2791, 2001.
- [19] Han, L.H., Yao, G.H., and Tao, Z., "Performance of concrete-filled thin-walled steel tubes under pure torsion", *Thin-Wall Structures*, vol.45, no. 1, pp. 24-36, 2007.
- [20] Nagy, N., Mohamed, M., Boot, J.C., "Nonlinear numerical modeling for the effects of surface explosions on buried reinforced concrete structures", *Geomechanics and Engineering*, vol. 2, no. 1, pp. 1-18, 2010.
- [21] Tao, Z., Wang, Z.B., and Yu, Q., "Finite element modelling of concrete-filled steel stub columns under axial compression", *Journal of Constructional Steel Research*, vol. 89, pp. 121-131, 2013.
- [22] Papanikolaou, V.K., and Kappos, A.J., "Confinement-sensitive plasticity constitutive model for concrete in triaxial compression", *International Journal of Solids and Structures*, vol. 44, no. 21, pp. 7021-7048, 2007.
- [23] Seow, P.E.C, and Swaddiwudhipong, S., "Failure surface for concrete under multiaxial load – a unified approach", *Journal of Materials in Civil Engineering*, vol. 17, no. 2, pp. 219-228, 2005.